Article

Coupled Fluorometer-Potentiostat System and Metal-Free Monochromatic Luminophores for High-Resolution Wavelength-Resolved Electrochemiluminescent Multiplex Bioassay

Yanqin Lv, Zhixin Zhou, Yanfei Shen, Qing Zhou, Jingjing Ji, Songqin Liu, and Yuanjian Zhang

ACS Sens., **Just Accepted Manuscript** • DOI: 10.1021/acssensors.8b00292 • Publication Date (Web): 08 Jun 2018

Coupled Fluorometer-Potentiostat System and Metal-Free Monochromatic Luminophores for High-Resolution Wavelength-Resolved Electrochemiluminescent Multiplex Bioassay

Yanqin Lv, Zhixin Zhou, Yanfei Shen, Qing Zhou, Jingjing Ji, Songqin Liu, Yuanjian Zhang*

Jiangsu Engineering Laboratory of Smart Carbon-Rich Materials and Device, Jiangsu Province Hi-Tech Key Laboratory for Bio-Medical Research, School of Chemistry and Chemical Engineering, Medical School, Southeast University, Nanjing 211189, China, Email: Yuanjian.Zhang@seu.edu.cn

ABSTRACT: The sensitive simultaneous detection of multiple biomarkers is critical for the early diagnosis of diseases. Among them, electrochemiluminescence (ECL) offers outstanding advantages, e.g. low background, over other optical sensing techniques. However, multiplexed ECL bioassay is hindered by not only the lack of generally available ECL spectrometers but also the limited number of biocompatible monochromatic ECL luminophores for decades. Herein, we report the addressing of these issues by re-examination of the recent tabletop spectrofluorometer coupled potentiostat as a high-resolution ECL spectrum acquisition system and using carbon nitrides as monochromatic luminophores. A wavelength-resolved multiplexing ECL biosensor is demonstrated to simultaneously detect CA19-9 and mesothelin, two pancreatic cancer biomarkers, at a single-electrode interface. This work could initiate new opportunities for more general multiplex ECL biosensors with competitive performances.

Keywords: Electrochemiluminescent spectrum, Simultaneous multiple biomarkers detection, Monochromatic luminophore, Carbon nitride, Coupled instruments

Because of the limited specificity of single biomarkers in disease diagnosis, the developing methods of multiple biomarkers detection is a major goal of bioanalytical chemistry to minimize false positives.[1-3] Electrochemiluminescence (ECL) offers several outstanding advantages over other optical sensing techniques, e.g., compared with photoluminescence, ECL has no background optical interference, whereas compared with chemiluminescence, ECL offers easier reaction control via applying different potentials and good temporal/spatial control.[4-8] Thus, ECL has attracted considerable attention in bioanalysis.[9-17] According to the fundamental theory of ECL, multiple luminophores can be distinguished by the potential required for excitation or by the wavelength of emission.[18] Potential-resolved ECL biosensors have been well developed[19-22] because of easy controlling of the potential for ECL reactions. By contrast, although the emission wavelength has more conceivable room for modulation, only very few works have demonstrated the direct utilization of ECL emission at different wavelengths. Homemade ECL spectrum acquisition systems were proposed, which consists of a photomultiplier tubes or charge-coupled device, a grating, and other complicated optical components.[7, 23-28] However, the construction of such a system is costly and requires extensive expertise. Alternatively, commercial spectrofluorometer coupled potentiostat for acquiring ECL spectra has been sporadically reported.[29] Nevertheless, their practical use has largely been hindered by either the high cost of modular spectrofluorometers[30] or the low sensitivity of portable spectrofluorometers to ultra-weak ECL emission.[29] Hence, ECL spectra were often obtained by using a ECL analyzer that recorded only the ECL intensity, supplementary with band-pass optical filters,[31] making the resolution rather low. Moreover, but not less important, the limited number of biocompatible monochromatic ECL luminophors is another bottleneck for ECL multiplex bioassay.[32] These are likely the main reasons why the wavelength-resolved ECL assay has not been extensively explored for decades thus far. Thanks to the utilization of techniques, such as the photon counting signal collection method, the sensitivity of nowadays tabletop spectrofluorometers that are available in many laboratories is substantially improved. However, such high sensitivity has been overlooked for ECL studies, and NOT been realized for ultra-weak ECL spectrum acquiring so far. Herein, we report the addressing of these issues by re-examination of the recent tabletop spectrofluorometer coupled potentiostat as an ECL spectrum acquisition system and using carbon nitrides as monochromatic luminophores.

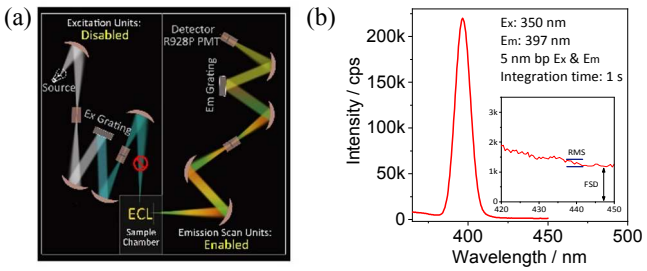

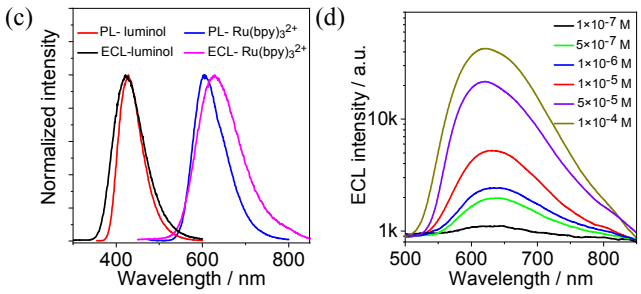

Figure 1. (a) Scheme of tabletop spectrofluorometer-potentiostat system for high-resolution ECL spectrum collection, and the diagram of the light path. (b) The water Raman signal recorded by the tabletop spectrofluorometer used in this study. (c) The ECL and PL spectra of luminol (5×10^{-4} M) and $Ru(bpy)_3^{2+}$ (1×10^{-5} M). (d) ECL spectra of $Ru(bpy)_3^{2+}$ with different concentration. Electrolytes for luminol: 0.01 M PBS (pH 7.4) containing 10 mM H_2O_2. Bias potential: 0.5 V. Electrolytes for $Ru(bpy)_3^{2+}$: 0.1 M PBS (pH 8.0) containing 0.1 M $K_2S_2O_8$.

RESULTS AND DISCUSSION

Figure 1a shows the general setup and optical path diagram of the ECL spectrum acquisition system that consisted of a tabletop spectrofluorometer and a potentiostat. Because of the utilization of techniques, such as the photon counting signal collection method, the sensitivity of the recent tabletop spectrofluorometers has been substantially improved, but historically overlooked for ECL studies and not been realized for ultra-weak ECL spectrum acquiring so far. The sensitivity, evaluated by the water Raman S/N values via RMS and FSD methods, was ca. 28,000 and 6,000, respectively (Figure 1b, see additional details in the SI), up to 10 times higher than that of the last generation of lower-performance spectrofluorometers often using analog detection. Such high sensitivity was favor of acquiring high-resolution ECL spectra, especially for the low-light-level detection. Notably, such instruments can be realized even when only a modest budget and limited expertise are available. To validate the feasibility of this spectrofluorometer-potentiostat system, the ECL spectra of traditional luminophores were collected. Figure 1c shows the high-resolution ECL spectra of luminol and $Ru(bpy)_3^{2+}$, which matched well with their photoluminescence (PL) spectra. The slight shifts are ascribed to the different internal conversion and/or vibration relaxation processes of the excited states of luminol and $Ru(bpy)_3^{2+}$ in ECL and PL.

Moreover, ECL spectra of $Ru(bpy)_3^{2+}$ with different concentrations were investigated. As shown in Figure. 1d, the lowest [$Ru(bpy)_3^{2+}$] that this instrument can detect for practical application under this experimental condition was 1×10^{-7} M, which also already reached the minimum range of the practical detection limit by conventional ECL analyzer that recorded only the ECL intensity (see Figure S1 and more discussion in SI). It is comparable the conventional concentration in previous studies (0.1 μM ~ 5 mM) [7, 13, 33-34], indicating the proposed ECL spectrum acquiring system had a very promising high sensitivity for ultra-weak emission detection.

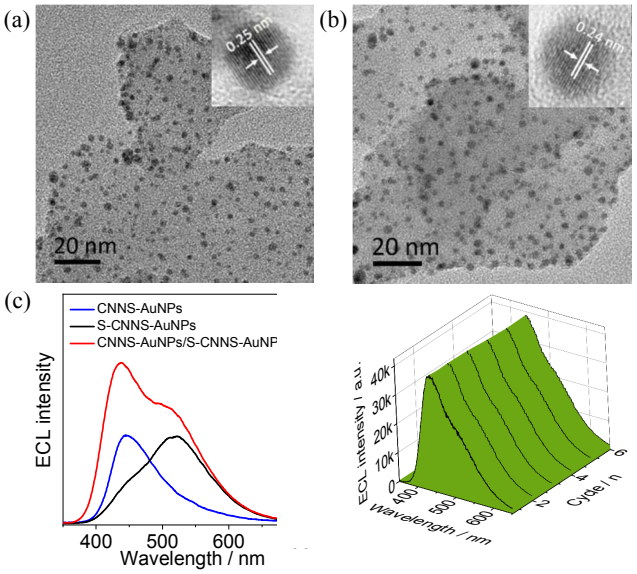

Figure 2. TEM images of CNNS-AuNPs (a) and S-CNNS-AuNPs (b); inset: HRTEM images. ECL spectra of CNNS-AuNPs, S-CNNS-AuNPs, and CNNS-AuNPs/S-CNNS-AuNPs at the single-electrode interface (c). ECL stability of CNNS-AuNPs/S-CNNS-AuNPs obtained by multiple measurements. Electrolyte: 0.01 M PBS (pH 7.4) containing 0.1 M $K_2S_2O_8$. Bias potential: −1.6 V.

As an emerging luminophore, carbon nitride demonstrate the advantages of low-cost, high biocompatibility and stability, easy functionalization, strong ECL activity, and an unambiguous luminescence mechanism.[35-38] Compared with heavy metal-containing quantum dots such as CdS and CdTe,[39] CNNS are metal-free; consequently, many ECL biosensors based on carbon nitride nanosheets (CNNS) have been developed, with very promising performances.[40-45] Moreover, our group recently reported the preparation of a diverse range of carbon nitrides with different nanostructures and dopants, which demonstrated different ECL emission wavelengths.[41] To ensure an intimate connection between nanosheets with biomolecules, as shown in TEM and HRTEM images (Figure 2a-b) and in the EDS elemental analysis results (Figure S2), Au nanoparticles (AuNPs) were homogeneously deposited onto CNNS and sulfur-doped CNNS (S-CNNS). It was attributed to an abundance of N-atoms in the framework of carbon nitride that offered active anchoring sites.[46] Figure 2c shows the ECL spectrum of CNNS-AuNPs on glassy carbon electrode (GCE) with a peak at 435 nm; by contrast, the ECL emission peak of S-CNNS-AuNPs red-shifted ca. 100 nm to 531 nm. Such large peak-shift was preferred for wavelength-resolved ECL bioassay. Notably, the ECL of CNNS-AuNPs and S-CNNS-AuNPs was stable with continuous electrochemical excitation and had similar excitation potentials (Figure S3), suggesting that their ECL could be achieved by the same bias potential, i.e., −1.6 V (Figure S4), when they are co-immobilized on the same electrode, a favor factor for instruments minimization.

For multiplex bioassay, CNNS-AuNPs and S-CNNS-AuNPs were further co-immobilized on a single GCE as monochromatic luminophores. As shown in Figure 2c, although the ECL emissions of CNNS-AuNPs and S-CNNS-AuNPs were partially overlapped, no evident quenching was observed at the single-electrode interface. This lack of quenching indicates that

no energy transfer occurred between them—an important prerequisite for the simultaneous wavelength-resolved sensing of multiple biomarkers. Moreover, only a minor standard deviation of 0.54% of the ECL spectrum was observed in six independent measurements, implying good reliability of the dual ECL luminophores at a single-electrode interface (Figure 2d).

Because the incidence of pancreatic ductal adenocarcinoma (PDAC, a major type of pancreatic cancer) approaches the patient mortality rate, the quest for an economic and reliable method of early detection of PDAC has continually attracted broad interest.[47] The combination of multiple appropriate biomarkers is generally accepted to enhance the specificity for the detection.[1-3] As an example, mixture of two typical PDAC biomarkers, e.g., CA19-9 and mesothelin (MSLN),[48-49] were analyzed by the proposed wavelength-resolved multiplexing ECL bioassay. Figure 3 illustrates the assembly process for the multiplexing ECL biosensor (see Figure S5 and further discussion in SI). Briefly, CNNS-AuNPs and S-CNNS-AuNPs were deposited onto a GCE. Then, anti-CA19-9 and anti-MSLN were assembled mostly via Au-S bonding, separately. Lastly, the CNNS-AuNPs/anti-CA19-9 and S-CNNS-AuNPs/anti-MSLN co-modified GCE was incubated in the solution containing the targeted CA19-9 and MSLN after blocking nonspecific adsorption sites with BSA(see detailed information in SI).

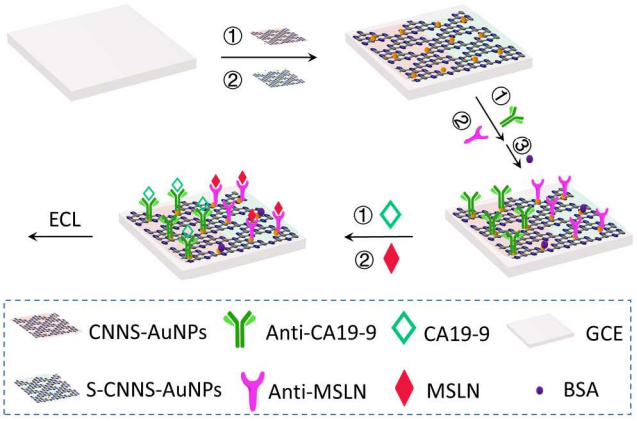

Figure 3. General assembly procedure for the wavelength-resolved ECL biosensor for the simultaneous detection of multiple biomarkers.

To demonstrate the feasibility of the proposed multiplexing ECL biosensor, two sets of experiments were undertaken. The concentration of MSLN was first fixed at 0 μg mL^{-1}, and the ECL spectra of the as-constructed immunosensor toward different concentrations of CA19-9 were monitored. The ECL intensity at 438 nm, which was mainly the contribution of CNNS, decreased with increasing CA19-9 concentration (Figure 4a). The linear relationship (Figure 4b, red fitted line, R^2 = 0.986) between the ECL intensity $[(I_0 - I)/I_0]$ at 438 nm and the concentration is described by

$$I_{CNNS-438} = 0.0515 \lg C_{CA19-9} + 0.3357 \quad (1)$$

For the minor ECL intensity change at 510 nm, which could be ascribed to the emission trailing edge of CNNS (Figure 4a), the equation of the linear calibration curve (Figure 4b, black fitted line, R^2 = 0.978) was found to be

$$I_{CNNS-510} = 0.014 \lg C_{CA19-9} + 0.1188 \quad (2)$$

The linear CA19-9 concentration range was from 0.01 to 80 U mL^{-1}.

In the second set of experiments, the concentration of CA19-9 was set as 0 U mL^{-1} and the ECL spectra of the as-constructed immunosensor toward different concentrations of MSLN were measured (Figure 4c). Similarly, the major and minor ECL intensity changes at 510 nm (Figure 4d, red fitted line, R^2 = 0.994) and 438 nm (Figure 4d, black fitted line, R^2 = 0.996)) are described by

$$I_{S-CNNS-510} = 0.0407 \lg C_{MSLN} + 0.3499 \quad (3)$$

$$I_{S-CNNS-438} = 0.014 \lg C_{MSLN} + 0.1724 \quad (4)$$

where the linear MSLN concentration range was from 0.001 to 50 μg mL^{-1}. The sensitivity of other methods and ours as well are summarized in Table 1. It can be seen that our method exhibited very competitive performance, considering that all these previous reports were devoted to single biomarker sensing while ours is more challenging and is for simultaneous detection of two biomarker. Moreover, in this concept of proof study, the biosensing interfaces was not fully optimized, for instance, it is highly expected that if the signal-amplification techniques[50] were used, the sensitivity would be further improved. Notably, these equations were found to also be applicable when CA19-9 and MSLN were spiked in human serum instead of PBS, indicating the high specificity of the proposed multiplex ECL biosensor (see recovery test in Table 2).

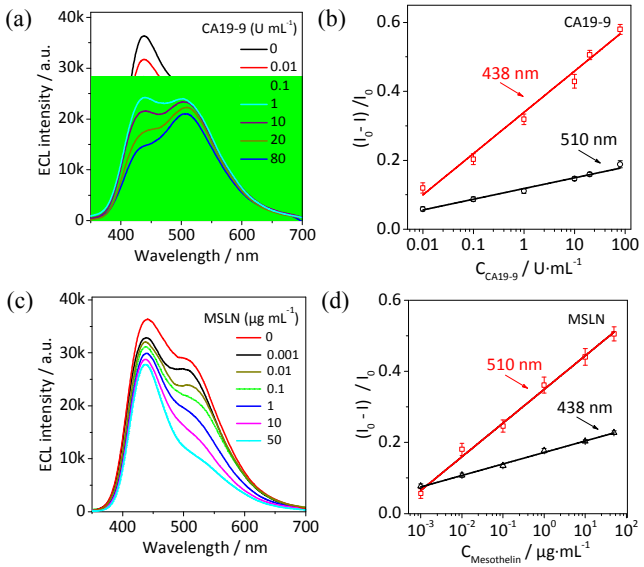

Figure 4. ECL spectra of the immunosensor in the presence of merely CA19-9 (a) or MSLN (c) at different concentrations. The calibration curves between ECL intensity (for 438-nm and 510-nm peaks) and CA19-9 (b) and MSLN (d) concentration. Electrolyte: 0.01 M PBS (pH 7.4) containing 0.1 M $K_2S_2O_8$. Bias potential: −1.6 V.

From these two sets of experiments, because of the minor crosstalk between the ECL spectra of CNNS and S-CNNS, four calibration curves between the ECL intensity (at the 438-nm peak and 510-nm peak) and concentration of the biomarkers (CA19-9 and MSLN) were obtained (Eqs. 1-4). In this context, a spectral crosstalk correction was applied to the four aforementioned calibration curves to simplify the practical multiplexed biomarker protein detection. In principle, the relationship between the ECL intensity of CNNS and the con-

centrations of CA19-9 and MSLN can be demonstrated as a multivariate linear algebraic equation:

$$I_{438} = f_1(C_{CA19\text{-}9}, C_{MSLN}) = I_{CNNS\text{-}438} + I_{S\text{-}CNNS\text{-}438} \quad (5)$$

Similarly, the ECL emission of S-CNNS can be described as

$$I_{510} = f_2(C_{CA19\text{-}9}, C_{MSLN}) = I_{CNNS\text{-}510} + I_{S\text{-}CNNS\text{-}510} \quad (6)$$

Using Eqs. 1-4, we deduced the following theoretical linear equations:

$$I_{438} = 0.0515 \lg C_{CA19\text{-}9} + 0.014 \lg C_{MSLN} + 0.5081 \quad (7)$$

$$I_{510} = 0.014 \lg C_{CA19\text{-}9} + 0.0407 \lg C_{MSLN} + 0.4687 \quad (8)$$

Thus, with mere measurement of the ECL intensities at 438 nm and 510 nm, the concentrations of CA19-9 and MSLN can be calculated using the proposed multiplexing ECL biosensing system. On this basis, to investigate the applicability of the biosensor under more complex conditions, we applied it to the simultaneous detection of spiked serum samples containing both CA19-9 and MSLN. Figure 5 shows the ECL spectra of the immunosensor for the simultaneous detection of CA19-9 and MSLN at different concentrations. As summarized in Table 1, the recoveries of CA19-9 and MSLN ranged from 95% to 105%, indicating good accuracy and high precision. In addition, the proposed multiplex ECL assay had excellent specificity in the presence of various interferents (Figure. S6). Therefore, this multiplex biosensing based on high-resolution wavelength-resolved ECL holds great potential for the clinical diagnosis.

Nevertheless, it is noted that the overlap between the ECL emissions of CNNS-AuNPs and S-CNNS-AuNPs may have negative interference for multiplexed bioassay. Indeed, this is a challenge for wavelength-resolved ECL bioassay, due to the limited types of biocompatible monochromatic luminophores. In general, there are two ways to eliminate such signal interference as much as possible. One is to prepare new ECL luminophores with large emission wavelength difference, which needs more depth future studies. The other one is to optimize the amount of current available CNNS-AuNPs and S-CNNS-AuNPs on the electrode, thus making a well balance between the major ECL emission peaks of them. In this context, 3 μL of CNNS-AuNPs and 10 μL of S-CNNS-AuNPs suspension were deposited on the electrode(see Figure S7 and more discussion in SI). Moreover, a spectral crosstalk correction was applied to the four aforementioned calibration curves (e.q. 1-4) to simplify the practical multiplexed biomarker protein detection.

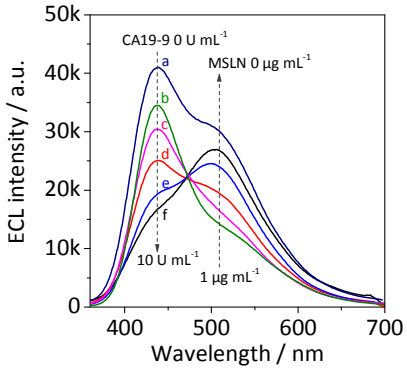

Figure 5. ECL spectra for the simultaneous detection of CA19-9 and MSLN at various concentrations: CA19-9 (a) 0, (b) 0.01, (c) 0.1, (d) 1 (e) 5.0, and (f)10 U mL^{-1}; MSLN (a) 0, (b) 10, (c) 1, (d) 0.1, (e) 0.01, and (f) 0.001 μg mL^{-1}. Electrolyte: 0.01 M PBS (pH 7.4) containing 0.1 M $K_2S_2O_8$. Bias potential: −1.6 V.

In summary, we report a wavelength-resolved ECL biosensor for the simultaneous detection of multiple biomarkers at a single-electrode interface. To this end, a high-resolution ECL spectrum acquisition system was proposed by re-examination of coupling the recent tabletop spectrofluorometer with much improved sensitivity and potentiostat. Moreover, the CNNS with different emission wavelengths were explored as metal-free monochromatic luminophores with premium properties, such as the same co-reagent and excitation potential for instrument minimization. The proposed ECL biosensor demonstrated good accuracy and high precision in the simultaneous detection of multiple PDAC biomarkers in spiked serum. Notably, the proposed instruments and monochromatic luminophores can be realized even when only a modest budget and limited expertise are available. This work would greatly pave the studies of less explored high-resolution wavelength-resolved ECL during the last few decades for multiplex bioassay with competitive performances.

ASSOCIATED CONTENT

Supporting Information

Experimental, EDS, ECL, EIS, CV curves and more control results and supplementary discussion. This material is available free of charge via the Internet at http://pubs.acs.org

AUTHOR INFORMATION

Corresponding Author

Yuanjian.Zhang@seu.edu.cn

ACKNOWLEDGMENT

This work was supported by the National Natural Science Foundation of China (21775018, 21675022), the Natural Science Foundation of Jiangsu Province (BK20160028, BK20170084), the Open Funds of the State Key Laboratory of Electroanalytical Chemistry (SKLEAC201703) and the Fundamental Research Funds for the Central Universities.

Table 1 Comparison of different methods for assay of CA19-9 and MSLN.

Targets	Methods	Linear range	LOD	Refs
CA19-9 (U/mL)	Monosaccharide imprinted sensor /Polysaccharide imprinted sensor	1–50/0.1–5	0.17/0.028	[51]
	Polarizationmodulated infrared reflection absorption spectroscopy	0.05–60	0.35	[52]
	Photoelectrochemistry	0.01–200	0.0039	[53]
	Impedance Spectroscopy	—	0.69	[54]
	Electrochemistry	5–100	1.6	[55]
	Multiplex electrochemiluminescence	0.01–80	0.083	This work
MSLN (μg/mL)	ELISA	0.081 – 5.2 ng/mL	—	[56]
	ELISA	0.005 – 0.05	0.005	[57]
	Multiplex electrochemiluminescence	0.001 – 50	0.00091	This work

Table 2. Recovery results for the detection of CA19-9 and MSLN in human serum samples

Sample	CA19-9 ($U \cdot mL^{-1}$)		MSLN ($\mu g \cdot mL^{-1}$)		Relative standard deviation		Recovery (%)	
	Added	Found	Added	Found	CA19-9	MSLN	CA19-9	MSLN
C1	1	0.92	0	N.D.	3.7	N.D.	92	N.D.
C2	10	9.8	0	N.D.	4	N.D.	98	N.D.
C3	20	20.4	0	N.D.	5.1	N.D.	102	N.D.
C4	40	38	0	N.D.	4.3	N.D.	95	N.D.
M1	0	N.D.	0.100	0.096	N.D.	4.5	N.D.	96
M2	0	N.D.	1.00	0.99	N.D.	5.0	N.D.	99
M3	0	N.D.	10.0	9.3	N.D.	3.4	N.D.	93
M4	0	N.D.	20.0	20.2	N.D.	4.2	N.D.	101
CM1	0.01	0.0095	1	0.99	3.5	4.1	95	99
CM2	0.1	0.101	0.1	0.103	5.0	3.9	101	103
CM3	1	0.98	0.01	0.0105	4.5	4.8	98	105
CM4	10	9.99	0.001	0.00098	3.9	4.4	99.9	98

REFERENCES

(1) Cohen, J. D.; Li, L.; Wang, Y.; Thoburn, C.; Afsari, B.; Danilova, L.; Douville, C.; Javed, A. A.; Wong, F.; Mattox, A., et al., Detection and localization of surgically resectable cancers with a multi-analyte blood test. *Science* **2018,** *359*, 926-930.

(2) He, X. P.; Hu, X. L.; James, T. D.; Yoon, J.; Tian, H., Multiplexed photoluminescent sensors: Towards improved disease diagnostics. *Chem. Soc. Rev.* **2017,** *46*, 6687-6696.

(3) Cohen, J. D.; Javed, A. A.; Thoburn, C.; Wong, F.; Tie, J.; Gibbs, P.; Schmidt, C. M.; Yip-Schneider, M. T.; Allen, P. J.; Schattner, M., et al., Combined circulating tumor DNA and protein biomarker-based liquid biopsy for the earlier detection of pancreatic cancers. *Proc. Natl. Acad. Sci. U.S.A.* **2017,** *114*, 10202-10207.

(4) Chen, Y.; Zhou, S.; Li, L.; Zhu, J., Nanomaterials-based sensitive electrochemiluminescence biosensing. *Nano Today* **2017,** *12*, 98-115.

(5) Liu, Z.; Qi, W.; Xu, G., Recent advances in electrochemiluminescence. *Chem. Soc. Rev.* **2015,** *44*, 3117-3142.

(6) Wu, P.; Hou, X.; Xu, J. J.; Chen, H. Y., Electrochemically generated versus photoexcited luminescence from semiconductor nanomaterials: Bridging the valley between two worlds. *Chem. Rev.* **2014,** *114*, 11027-11059.

(7) Miao, W., Electrogenerated chemiluminescence and its biorelated applications. *Chem. Rev.* **2008,** *108*, 2506-2553.

(8) Santhanam, K. S. V.; Bard, A. J., Chemiluminescence of electrogenerated 9, 10-diphenylanthracene anion radical. *J. Am. Chem. Soc.* **1965,** *87*, 139-140.

(9) Xing, H.; Zhai, Q.; Zhang, X.; Li, J.; Wang, E., Boron nitride quantum dots as efficient coreactant for enhanced electrochemiluminescence of ruthenium(ii) tris(2,2'-bipyridyl). *Anal. Chem.* **2018,** *90*, 2141-2147.

(10) Feng, Y.; Wang, N.; Ju, H., Highly efficient electrochemiluminescence of cyanovinylene-contained polymer dots in aqueous medium and its application in imaging analysis. *Anal. Chem.* **2018,** *90*, 1202-1208.

(11) Liu, S.; Yuan, H.; Bai, H.; Zhang, P.; Lv, F.; Liu, L.; Dai, Z.; Bao, J.; Wang, S., Electrochemiluminescence for electric-driven antibacterial therapeutics. *J. Am. Chem. Soc.* **2018,** *140*, 2284-2291.

(12) Nie, Y.; Zhang, P.; Wang, H.; Zhuo, Y.; Chai, Y.; Yuan, R., Ultrasensitive electrochemiluminescence biosensing platform for detection of multiple types of biomarkers toward identical cancer on a single interface. *Anal. Chem.* **2017,** *89*, 12821-12827.

(13) Irkham; Watanabe, T.; Fiorani, A.; Valenti, G.; Paolucci, F.; Einaga, Y., Co-reactant-on-demand ecl: Electrogenerated chemiluminescence by the in situ production of s2o8(2-) at boron-doped diamond electrodes. *J. Am. Chem. Soc.* **2016,** *138*, 15636-15641.

(14) Zhou, H.; Han, T.; Wei, Q.; Zhang, S., Efficient enhancement of electrochemiluminescence from cadmium sulfide quantum dots by glucose oxidase mimicking gold nanoparticles for highly sensitive assay of methyltransferase activity. *Anal. Chem.* **2016,** *88*, 2976-2983.

(15) He, Y.; Li, J.; Liu, Y., Reusable and dual-potential responses electrogenerated chemiluminescence biosensor for synchronously cytosensing and dynamic cell surface n-glycan evaluation. *Anal. Chem.* **2015,** *87*, 9777-9785.

(16) Qi, H.; Qiu, X.; Xie, D.; Ling, C.; Gao, Q.; Zhang, C., Ultrasensitive electrogenerated chemiluminescence peptide-based method for the determination of cardiac troponin i incorporating amplification of signal reagent-encapsulated liposomes. *Anal. Chem.* **2013,** *85*, 3886-3894.

(17) Xu, L.-l.; Zhang, W.; Shang, L.; Ma, R.; Jia, L.-p.; Jia, W.; Wang, H.; Niu, L., Perylenetetracarboxylic acid and carbon quantum dots assembled synergistic electrochemiluminescence nanomaterial for ultra-sensitive carcinoembryonic antigen detection. *Biosens. Bioelectron.* **2018,** *103*, 6-11.

(18) Doeven, E. H.; Barbante, G. J.; Hogan, C. F.; Francis, P. S., Potential-resolved electrogenerated chemiluminescence for the selective detection of multiple luminophores. *ChemPlusChem* **2015,** *80*, 456-470.

(19) Wang, Y. Z.; Xu, C. H.; Zhao, W.; Guan, Q. Y.; Chen, H. Y.; Xu, J. J., Bipolar electrode based multicolor electrochemiluminescence biosensor. *Anal. Chem.* **2017,** *89*, 8050-8056.

(20) Liu, X.; Jiang, H.; Fang, Y.; Zhao, W.; Wang, N.; Zang, G., Quantum dots based potential-resolution dual-targets electrochemiluminescent immunosensor for subtype of tumor marker and its serological evaluation. *Anal. Chem.* **2015,** *87*, 9163-9169.

(21) Han, F.; Jiang, H.; Fang, D.; Jiang, D., Potential-resolved electrochemiluminescence for determination of two antigens at the cell surface. *Anal. Chem.* **2014,** *86*, 6896-6902.

(22) Doeven, E. H.; Zammit, E. M.; Barbante, G. J.; Hogan, C. F.; Barnett, N. W.; Francis, P. S., Selective excitation of concomitant electrochemiluminophores: Tuning emission color by electrode potential. *Angew. Chem. Int. Ed.* **2012,** *51*, 4354-4357.

(23) Zou, G.; Tan, X.; Long, X.; He, Y.; Miao, W., Spectrum-resolved dual-color electrochemiluminescence immunoassay for simultaneous detection of two targets with nanocrystals as tags. *Anal. Chem.* **2017,** *89*, 13024-13029.

(24) Ma, C.; Wu, W.; Peng, Y.; Wang, M. X.; Chen, G.; Chen, Z.; Zhu, J. J., A spectral shift-based electrochemiluminescence sensor for hydrogen sulfide. *Anal. Chem.* **2017,** *90*, 1334-1339.

(25) Shu, J.; Han, Z.; Zheng, T.; Du, D.; Zou, G.; Cui, H., Potential-resolved multicolor electrochemiluminescence of n-(4-aminobutyl)-n-ethylisoluminol/tetra(4-carboxyphenyl)porphyrin/tio2 nanoluminophores. *Anal. Chem.* **2017,** *89*, 12636-12640.

(26) Zhang, X.; Tan, X.; Zhang, B.; Miao, W.; Zou, G., Spectrum-based electrochemiluminescent immunoassay with ternary cdznse nanocrystals as labels. *Anal. Chem.* **2016,** *88*, 6947-6953.

(27) Neves, M. M. P. S.; Bobes-Limenes, P.; Pérez-Junquera, A.; González-García, M. B.; Hernández-Santos, D.; Fanjul-Bolado, P., Miniaturized analytical instrumentation for electrochemiluminescence assays: A spectrometer and a photodiode-based device. *Anal. Bioanal. Chem* **2016,** *408*, 7121-7127.

(28) Staninski, K.; Kaczmarek, M.; Lis, S.; Komar, D.; Szyczewski, A., Spectral analysis in ultraweak emissions of chemi- and electrochemiluminescence systems. *J. Rare Earth.* **2009,** *27*, 593-597.

(29) Ramírez, M. G.; Díaz-García, M. A.; Montilla, F., Optimization of the electrochemically generated luminescence of polyfluorene films. *J. Phys. Chem. C* **2018,** *122*, 3608-3616.

(30) Chen, L.; Huang, D.; Ren, S.; Dong, T.; Chi, Y.; Chen, G., Preparation of graphite-like carbon nitride nanoflake film with strong fluorescent and electrochemiluminescent activity. *Nanoscale* **2013,** *5*, 225-230.

(31) Dai, P. P.; Yu, T.; Shi, H. W.; Xu, J. J.; Chen, H. Y., General strategy for enhancing electrochemiluminescence of semiconductor nanocrystals by hydrogen peroxide and potassium persulfate as dual coreactants. *Anal. Chem.* **2015,** *87*, 12372-12379.

(32) Rizzo, F.; Polo, F.; Bottaro, G.; Fantacci, S.; Antonello, S.; Armelao, L.; Quici, S.; Maran, F., From blue to green: Fine-tuning of photoluminescence and electrochemiluminescence in bifunctional organic dyes. *J. Am. Chem. Soc.* **2017,** *139*, 2060-2069.

(33) Miao, W.; Bard, A. J., Electrogenerated chemiluminescence. 77. DNA hybridization detection at high amplification with $[Ru(bpy)_3]^{2+}$-containing microspheres. *Anal. Chem.* **2004,** *76*, 5379-5386.

(34) Long, Y.-M.; Bao, L.; Zhao, J.-Y.; Zhang, Z.-L.; Pang, D.-W., Revealing carbon nanodots as coreactants of the anodic electrochemiluminescence of $Ru(bpy)_3^{2+}$. *Anal. Chem.* **2014,** *86*, 7224-7228.

(35) Zhou, Z.; Zhang, Y.; Shen, Y.; Liu, S.; Zhang, Y., Molecular engineering of polymeric carbon nitride: Advancing applications from photocatalysis to biosensing and more. *Chem. Soc. Rev.* **2018**.

(36) Ji, J.; Wen, J.; Shen, Y.; Lv, Y.; Chen, Y.; Liu, S.; Ma, H.; Zhang, Y., Simultaneous noncovalent modification and exfoliation of 2d carbon nitride for enhanced electrochemiluminescent biosensing. *J. Am. Chem. Soc.* **2017,** *139*, 11698-11701.

(37) Dong, Y.; Wang, Q.; Wu, H.; Chen, Y.; Lu, C. H.; Chi, Y.; Yang, H. H., Graphitic carbon nitride materials: Sensing, imaging and therapy. *Small* **2016,** *12*, 5376-5393.

(38) Zhang, X.; Xie, X.; Wang, H.; Zhang, J.; Pan, B.; Xie, Y., Enhanced photoresponsive ultrathin graphitic-phase c3n4 nanosheets for bioimaging. *J. Am. Chem. Soc.* **2013,** *135*, 18-21.

(39) Winnik, F. M.; Maysinger, D., Quantum dot cytotoxicity and ways to reduce it. *Accounts. Chem. Res.* **2013,** *46*, 672-680.

(40) Lv, Y.; Chen, S.; Shen, Y.; Ji, J.; Zhou, Q.; Liu, S.; Zhang, Y., Competitive multiple-mechanism-driven electrochemiluminescent detection of 8-hydroxy-2'-deoxyguanosine. *J. Am. Chem. Soc.* **2018,** *140*, 2801-2804.

(41) Zhou, Z.; Shang, Q.; Shen, Y.; Zhang, L.; Zhang, Y.; Lv, Y.; Li, Y.; Liu, S.; Zhang, Y., Chemically modulated carbon nitride nanosheets for highly selective electrochemiluminescent detection of multiple metal-ions. *Anal. Chem.* **2016,** *88*, 6004-6010.

(42) Shang, Q.; Zhou, Z.; Shen, Y.; Zhang, Y.; Li, Y.; Liu, S.; Zhang, Y., Potential-modulated electrochemiluminescence of carbon nitride nanosheets for dual-signal sensing of metal ions. *ACS Appl. Mater. Interfaces* **2015,** *7*, 23672-23678.

(43) Zhang, X. L.; Zheng, C.; Guo, S. S.; Li, J.; Yang, H. H.; Chen, G., Turn-on fluorescence sensor for intracellular imaging of glutathione using g-c(3)n(4) nanosheet-mno(2) sandwich nanocomposite. *Anal. Chem.* **2014,** *86*, 3426-3434.

(44) Tang, Y.; Song, H.; Su, Y.; Lv, Y., Turn-on persistent luminescence probe based on graphitic carbon nitride for imaging detection of biothiols in biological fluids. *Anal. Chem.* **2013,** *85*, 11876-11884.

(45) Cheng, C.; Huang, Y.; Tian, X.; Zheng, B.; Li, Y.; Yuan, H.; Xiao, D.; Xie, S.; Choi, M. M., Electrogenerated chemiluminescence behavior of graphite-like carbon nitride and its application in selective sensing cu2+. *Anal. Chem.* **2012,** *84*, 4754-4759.

(46) Zhang, Y.; Thomas, A.; Antonietti, M.; Wang, X., Activation of carbon nitride solids by protonation: Morphology changes, enhanced ionic conductivity, and photoconduction experiments. *J. Am. Chem. Soc.* **2009,** *131*, 50-51.

(47) Arasaradnam, R.; Wicaksono, A.; O'Brien, H.; Kocher, H. M.; Covington, J. A.; Crnogorac-Jurcevic, T., Non-invasive diagnosis of pancreatic cancer through detection of volatile organic compounds in urine. *Gastroenterology.* **2017**.

(48) Liu, J.; Gao, J.; Du, Y.; Li, Z.; Ren, Y.; Gu, J.; Wang, X.; Gong, Y.; Wang, W.; Kong, X., Combination of plasma micrornas with serum ca19-9 for early detection of pancreatic cancer. *Int. J. Cancer* **2012,** *131*, 683-691.

(49) Hassan, R.; Bera, T.; Pastan, I., Mesothelin:A new target for immunotherapy *Clin. Cancer. Res.* **2004,** *10*, 3937-3942.

(50) Lei, J.; Ju, H., Signal amplification using functional nanomaterials for biosensing. *Chem. Soc. Rev.* **2012,** *41*, 2122-2134.

(51) Li, J.; Ma, X.; Li, M.; Zhang, Y., Does polysaccharide is an idea template selection for glycosyl imprinting? *Biosens. Bioelectron.* **2018,** *99*, 438-442.

(52) Thapa, A.; Soares, A. C.; Soares, J. C.; Awan, I. T.; Volpati, D.; Melendez, M. E.; Fregnani, J.; Carvalho, A. L.; Oliveira, O. N., Jr., Carbon nanotube matrix for highly sensitive biosensors to detect pancreatic cancer biomarker ca19-9. *ACS Appl. Mater. Interfaces* **2017,** *9*, 25878-25886.

(53) Zhu, H.; Fan, G. C.; Abdel-Halim, E. S.; Zhang, J. R.; Zhu, J. J., Ultrasensitive photoelectrochemical immunoassay for ca19-9 detection based on cdse@zns quantum dots sensitized tio2nws/au hybrid structure amplified by quenching effect of ab2@v(2+) conjugates. *Biosens. Bioelectron.* **2016,** *77*, 339-346.

(54) Soares, A. C.; Soares, J. C.; Shimizu, F. M.; Melendez, M. E.; Carvalho, A. L.; Oliveira, O. N., Jr., Controlled film architectures to detect a biomarker for pancreatic cancer using impedance spectroscopy. *ACS Appl. Mater. Interfaces* **2015,** *7*, 25930-25937.

(55) Wang, G.; Qing, Y.; Shan, J.; Jin, F.; Yuan, R.; Wang, D., Cation-exchange antibody labeling for simultaneous electrochemical detection of tumor markers ca15-3 and ca19-9. *Microchimica Acta* **2013,** *180*, 651-657.

(56) Shiomi, K.; Miyamoto, H.; Segawa, T.; Hagiwara, Y.; Ota, A.; Maeda, M.; Takahashi, K.; Masuda, K.; Sakao, Y.; Hino, O., Novel elisa system for detection of n-erc/mesothelin in the sera of mesothelioma patients. *Cancer Sci* **2006,** *97*, 928-932.

(57) Hassan, R.; Remaley, A. T.; Sampson, M. L.; Zhang, J.; Cox, D. D.; Pingpank, J.; Alexander, R.; Willingham, M.; Pastan, I.; Onda, M., Detection and quantitation of serum mesothelin, a tumor marker for patients with mesothelioma and ovarian cancer. *Clin. Cancer. Res.* **2006,** *12*, 447-453.

Table of Contents artwork